EMBO reports

scientific report

A genetic screen identifies BRCA2 and PALB2 as key regulators of G2 checkpoint maintenance

Tobias Menzel[1], Viola Nähse-Kumpf[2], Arne Nedergaard Kousholt[1]*, Ditte Kjærsgaard Klein[1], Christin Lund-Andersen[2], Michael Lees[1], Jens Vilstrup Johansen[1], Randi G. Syljuåsen[2+] & Claus Storgaard Sørensen[1++]*

[1]Biotech Research and Innovation Centre, University of Copenhagen, Copenhagen, Denmark, and [2]Department of Radiation Biology, Institute for Cancer Research, Norwegian Radium Hospital, Oslo University Hospital, Oslo, Norway

To identify key connections between DNA-damage repair and checkpoint pathways, we performed RNA interference screens for regulators of the ionizing radiation-induced G2 checkpoint, and we identified the breast cancer gene *BRCA2*. The checkpoint was also abrogated following depletion of PALB2, an interaction partner of BRCA2. BRCA2 and PALB2 depletion led to premature checkpoint abrogation and earlier activation of the AURORA A–PLK1 checkpoint-recovery pathway. These results indicate that the breast cancer tumour suppressors and homologous recombination repair proteins BRCA2 and PALB2 are main regulators of G2 checkpoint maintenance following DNA-damage.

Keywords: siRNA screens; G2 checkpoint; DNA damage; BRCA2–PALB2; AURORA A/BORA/PLK1

EMBO *reports* (2011) **12**, 705–712. doi:10.1038/embor.2011.99

INTRODUCTION

In response to DNA damaging agents such as ionizing radiation, human cells activate cell-cycle checkpoints to delay cell-cycle progression and facilitate DNA repair. Cells exposed to ionizing radiation in S and G2 phase will arrest at the G2 checkpoint (Iliakis *et al*, 2003). This checkpoint inhibits cyclin B-CDK1 activity, the main driver of the G2-to-M cell-cycle transition. Inhibition of CDK1 is coordinated by the kinases ATM (ataxia-telangiectasia mutated) and ATR (ATM and Rad3 related) through phosphorylation of downstream targets such as CHK1 (Iliakis *et al*, 2003; Ciccia & Elledge, 2010). Following completion of DNA damage repair, the checkpoint is inactivated and CDK1 activity is restored to drive cell-cycle progression (van Vugt *et al*, 2005). This occurs through a process dependent on activation of PLK1, which is stimulated by AURORA A kinase and its activating partner BORA (van Vugt *et al*, 2004; Macurek *et al*, 2008). The upstream regulators of PLK1, AURORA A and BORA are not known.

As the G2 checkpoint is normally maintained until the damage has been repaired, the signalling cascades in control of this checkpoint and DNA repair are probably tightly coordinated. It is clear that checkpoint kinases, such as CHK1, regulate and stimulate repair pathways (Hu *et al*, 2005; Sørensen *et al*, 2005). However, it is not well understood whether DNA repair proteins can also control the restarting of the cell cycle following checkpoint arrest.

To identify new connections between DNA repair and checkpoint pathways, we developed a high-throughput assay to perform short-interfering RNA (siRNA) screens for unknown G2 checkpoint regulators following exposure to ionizing radiation. We identified the homologous recombination repair protein BRCA2 as an important regulator of G2 checkpoint maintenance, and BRCA2 functions together with its binding partner PALB2. These findings identify a new and main role of repair-pathway components in G2 checkpoint control.

RESULTS AND DISCUSSION

To perform siRNA screens for unknown G2 checkpoint regulators following ionizing radiation (Fig 1A), we considered the fact that histone H3 becomes phosphorylated on its Ser 10 residue during prophase and metaphase in mitosis (Hendzel *et al*, 1997). Cells were reverse transfected in 384-well plates with the siRNA library using three individually plated siRNAs per target. Two days after transfection, cells were irradiated with 6 Gy of ionizing radiation to induce the G2 checkpoint, and 2 h later the mitotic spindle inhibitor nocodazole was added and incubated for a further 8 hours to arrest cells that escape the checkpoint in mitosis (Fig 1A,B). siRNAs targeting CHK1 and the CHK1-inhibitor Gö6976 were used as positive controls in the screen (Fig 1C). Detection of H3Ser10p-positive cells was achieved by automated microscope image acquisition (Fig 1C, top), followed by statistical analysis to identify candidate genes (König *et al*, 2007). The screen was performed in the human osteosarcoma cell line U2OS expressing dominant-negative p53 (U2OS p53dneg). By inhibiting

[1]Biotech Research and Innovation Centre, University of Copenhagen, Ole Maaløes Vej 5, Copenhagen N 2200, Denmark
[2]Department of Radiation Biology, Institute for Cancer Research, Norwegian Radium Hospital, Oslo University Hospital, Oslo 0310, Norway
*These authors contributed equally to this work
[+]Corresponding author. Tel: +47 2278 1468; Fax: +47 2278 1495; E-mail: randi.syljuasen@rr-research.no
[++]Corresponding author. Tel: +45 3532 5678; Fax: +45 3532 5669; E-mail: css@bric.ku.dk

Received 1 March 2011; revised 18 April 2011; accepted 3 May 2011; published online 3 June 2011

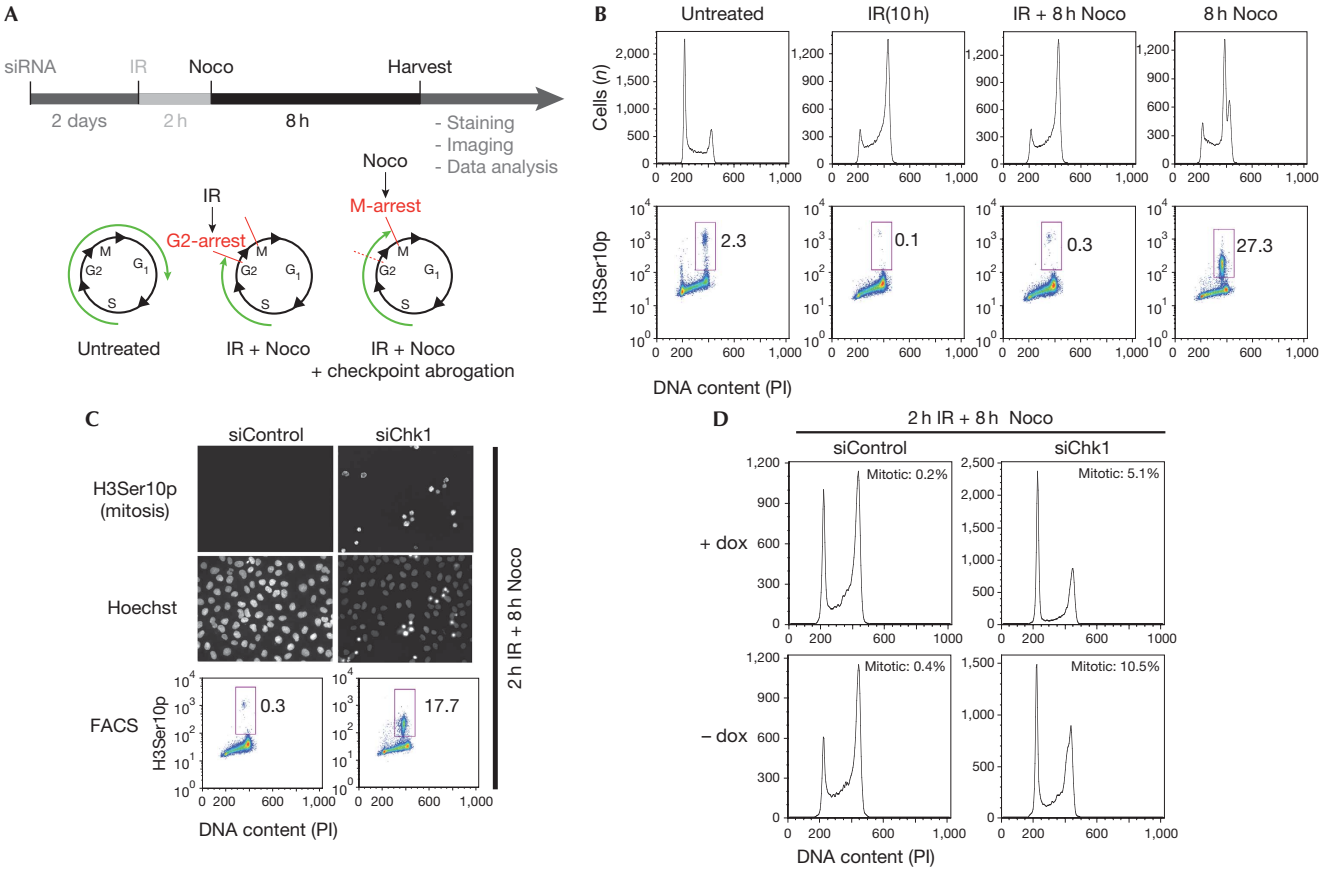

I

Gene symbol	siRNAs for run1	siRNAs for run2	p_run1	p_run2	p_fisherMethod
CHEK1	2	2	2.18×10^{-6}	2.18×10^{-6}	1.29×10^{-10}
WEE1	3	3	1.20×10^{-5}	2.66×10^{-6}	8.07×10^{-10}
MYT1	2	1	0.001847895	0.030445645	0.000606797
EPHA5	1	1	0.010817216	0.005418412	0.000629762
ALS2CR2	2	1	0.00231532	0.084361511	0.001863556
MGC42105	2	1	0.00272636	0.099631265	0.002502008
LYN	1	2	0.060266975	0.004558462	0.002527396
ACVRL1	1	2	0.1097162	0.00272636	0.002726426
PRKCD	1	1	0.021556141	0.014405543	0.002818735
MAP3K10	1	1	0.019771745	0.021556141	0.003733788
PLCB4	1	1	0.033986316	0.016196447	0.00468151
CDC42BPB	1	1	0.017985181	0.033986316	0.005134503

◀ **Fig 1** | High-throughput siRNA screen identifies kinases that regulate the ionizing-radiation-induced G2 checkpoint. (**A**) Schematic overview of the robot-automated high-throughput siRNA screen. p53 dominant-negative U2OS (U2OS p53dneg) cells were reverse transfected and, after incubation for 2 days, treated with 6 Gy of IR and, 2 h later, with nocodazole for 8 h and subsequently stained with H3Ser10p antibody to stain mitotic cells, and Hoechst to stain the nuclei. (**B**) Flow cytometric analysis of U2OS p53dneg cells. Where indicated, cells were treated with IR (6 Gy) and 2 h later with nocodazole for 8 h. Cells were collected and stained with phospho H3ser10 (H3Ser10p) antibody and propidium iodide (PI). (**C**) CHK1 depletion abrogates the G2 checkpoint. U2OS p53dneg cells were transfected with CHK1 siRNA and treated with IR (6 Gy) and 2 h later with nocodazole for 8 h. Top panel: immunofluorescence microscopy images obtained from the robot-automated screen. Bottom panel: cells were collected and processed for flow cytometric analysis as in **B**. (**D**) Parental U2OS cells partly arrest in G1 after DNA damage and CHK1 depletion. U2OS p53dneg cells were grown in the presence (+dox) and absence (−dox) of doxycycline. In the absence of doxycycline, a dominant-negative p53 is expressed and this represses p53 function. Cells were transfected with CHK1 siRNA for 2 days and treated with 6 Gy of IR and 2 h later with nocodazole for 8 h, or left untreated before collecting and staining for H3Ser10p and PI. Mitotic cells were determined as the percentage of H3Ser10p-positive cells. (**E**) Scatterplot showing siRNA log2 values for screen run 1 compared with run 2. Positive and negative controls highlighted in grey and red, respectively. (**F**) Plot of the strictly standardized mean difference (SSMD) for the kinome screens. For each plate (*x* axis) the SSMD is plotted for both screen 1 (circles) and screen 2 (triangles). Value over 2 indicate acceptable quality of the plate. (**G**) Calculated *z*-score for each siRNA screen with positive and negative controls highlighted in red and green, respectively. (**H**) Genes were ranked according to their RSA-derived *P*-value. The positions of CHK1 and WEE1 are indicated by red crosses. (**I**) The top-scoring genes from the screen. Genes are ranked according to their combined *P*-value using Fisher's method. The RSA *P*-values and the number of scoring siRNAs are also indicated. FACS, fluorescence-activated cell sorting; IR, ionizing radiation; Noco, nocodazole; RSA, redundant siRNA analysis; siRNA, short-interfering RNA.

p53, an important activator of the G1/S checkpoint (Iliakis *et al*, 2003), the number of cells reaching the G2 checkpoint was increased (Fig 1D).

To validate our high-throughput assay, we performed the screen twice using an siRNA library targeting the human kinome (see supplementary Table S1 online). Most siRNAs showed similar phenotypes in the two screens (Fig 1E). As quality metrics, we calculated the strictly standardized mean difference for the plates, which showed little variation (Fig 1F; Birmingham *et al*, 2009). Heatmaps of the raw scores (or ranks) of the 384 wells were made to exclude any spatial bias (data not shown). We also calculated the *z*-score and robust *z*-score (when applicable) for each siRNA (Birmingham *et al*, 2009). The positive and negative controls separated well, and few siRNAs induced mitotic accumulation (Fig 1G). CHK1 and the CDK1-inhibiting kinases WEE1 and MYT1 were identified; all three are known G2-checkpoint activators (Boutros *et al*, 2006; Sørensen *et al*, 2010; Fig 1H,I). This confirmed that our new screen efficiently identifies checkpoint regulators. In addition, nine kinases that have not been previously recognized as checkpoint regulators were identified as candidates. We noted that several kinases with known checkpoint roles were not identified in our screens, such as ATR, which highlights that siRNA screens are unlikely to be able to elucidate entire pathways, due to issues such as siRNA-knockdown efficacy.

To identify DNA repair factors with a regulatory role in the ionizing-radiation-induced G2 checkpoint, we next performed similar screens using a custom-made siRNA library targeting human DNA repair factors (see supplementary Table S1 online). The screen was conducted twice, and the results were highly reproducible, with little plate-to-plate variation (supplementary Fig S1 online). As in the kinome screen, few siRNAs led to G2 checkpoint abrogation (Fig 2A,B). All three siRNAs of BRCA2 scored highly (Fig 2C). The role of BRCA2 in the G2/M checkpoint is unknown (Venkitaraman, 2009). To validate the findings of the screens and exclude possible off-target effects of the siRNA, we transfected cells with the three screen-derived siRNAs targeting BRCA2. All three siRNAs abrogated the G2 checkpoint (Fig 2D) and depleted BRCA2 (Fig 2E). Similar G2 checkpoint abrogation was seen with BRCA2 siRNA concentrations ranging from 5 to 100 nM (data not shown), or with BRCA2 depletion by endoribonuclease-prepared siRNA (date not shown). Importantly, BRCA2-depleted cells did not arrest within mitosis, which would have affected our analysis (supplementary Fig S3 online, white and light grey bars, 8 h Noco). BRCA2 also abrogated the G2 checkpoint in p53 wild-type TIG-3-tert cells (Fig 2F), and in $p53^{-/-}$ HCT116, HeLa and parental U2OS cells (supplementary Fig S2 online).

The G2 checkpoint arrest was initially activated after BRCA2 knockdown, which was clear from the low mitotic index 1 and 2 h after exposure to ionizing radiation (Fig 3A), as well as proficient CHK1 phosphorylation and CDC25A downregulation (Fig 3D). However, at later time points after exposure to ionizing radiation, BRCA2-depleted cells overcame the G2 arrest, indicating that BRCA2 has a role in checkpoint maintenance, rather than activation (Fig 3A). BRCA2-depleted cells entering mitosis after ionizing radiation eventually proceed to G1 phase in the absence of the nocodazole trap (supplementary Movies 1 and 2 online). To examine whether cells entering mitosis in the absence of BRCA2 contain unrepaired DNA damage, we stained cells for γH2AX, an established DNA damage marker (Bonner *et al*, 2008). BRCA2-depleted cells that were captured in mitosis after exposure to ionizing radiation and nocodazole treatment were γH2AX-positive, similarly to CHK1-depleted cells receiving the same treatment (Fig 3B,C), and they showed condensed chromatin typical of mitotic cells (Fig 3C). Thus, cells enter mitosis in the absence of BRCA2 despite persisting DNA-damage signals. Next, we asked whether BRCA2-deficient cells entering mitosis after exposure to ionizing radiation were cells that had overcome the S-phase arrest, which would suggest that BRCA2 affects the intra-S checkpoint. To distinguish between cells that were in S phase and G2 phase at the point of irradiation, we pulsed the cells with the nucleotide analogue EdU before ionizing radiation/nocodazole treatment. The fraction of the cells accumulating in mitosis after exposure to ionizing radiation and BRCA2 depletion were mostly EdU negative (Fig 3E), confirming that BRCA2 affected G2-phase cells. These results were supported by experiments using the DNA polymerase inhibitor aphidicolin to arrest S-phase cells (Deckbar *et al*, 2007). In the presence of aphidicolin, BRCA2-depleted cells were able to enter mitosis after exposure to ionizing radiation,

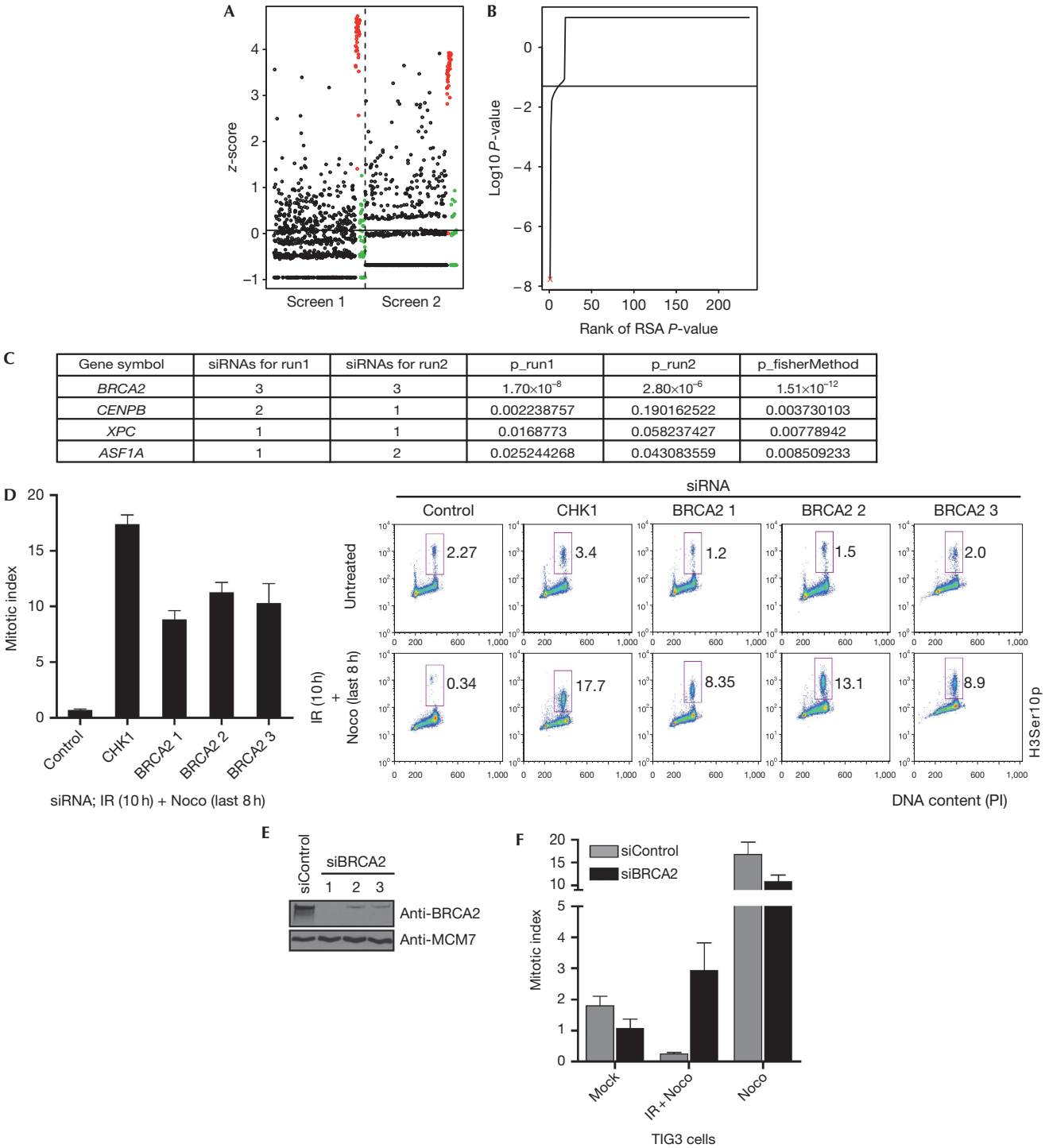

Gene symbol	siRNAs for run1	siRNAs for run2	p_run1	p_run2	p_fisherMethod
BRCA2	3	3	1.70×10^{-8}	2.80×10^{-6}	1.51×10^{-12}
CENPB	2	1	0.002238757	0.190162522	0.003730103
XPC	1	1	0.0168773	0.058237427	0.00778942
ASF1A	1	2	0.025244268	0.043083559	0.008509233

Fig 2 | High-throughput siRNA screen identifies BRCA2 as a main regulator of the ionizing-radiation-induced G2 checkpoint. (**A**) Calculated *z*-score for each siRNA screen with positive and negative controls highlighted in red and green, respectively. (**B**) Genes were ranked according to their RSA-derived *P*-value. The position of BRCA2 is indicated (red cross). (**C**) The top-scoring genes from the screen. Genes are ranked according to their combined *P*-value using Fisher's method. (**D**) U2OS p53dneg cells were transfected with three siRNAs targeting BRCA2 and CHK1, respectively. After 2 days they were treated with 6 Gy of IR, 2 h later with nocodazole for 8 h and processed for flow cytometric analysis. The bar plot is the mean of the percentage of H3Ser10p-positive cells of three experiments. Error bars indicate s.e.m. ($n = 3$). (**E**) Immunoblot of cells treated as in **D**. (**F**) TIG3-tert cells were transfected with control (grey) and BRCA2 (black) siRNA, respectively, for 2 days, treated with 6 Gy of IR and 1 h later with Nocodazole for 6 h and analysed by flow cytometry. Error bars indicate s.e.m. ($n = 3$). H3Ser10p, phospho-H3Ser10p; IR, ionizing radiation; Noco, nocodazole; siRNA, short-interfering RNA; U2OS p53dneg, p53 dominant-negative U2OS.

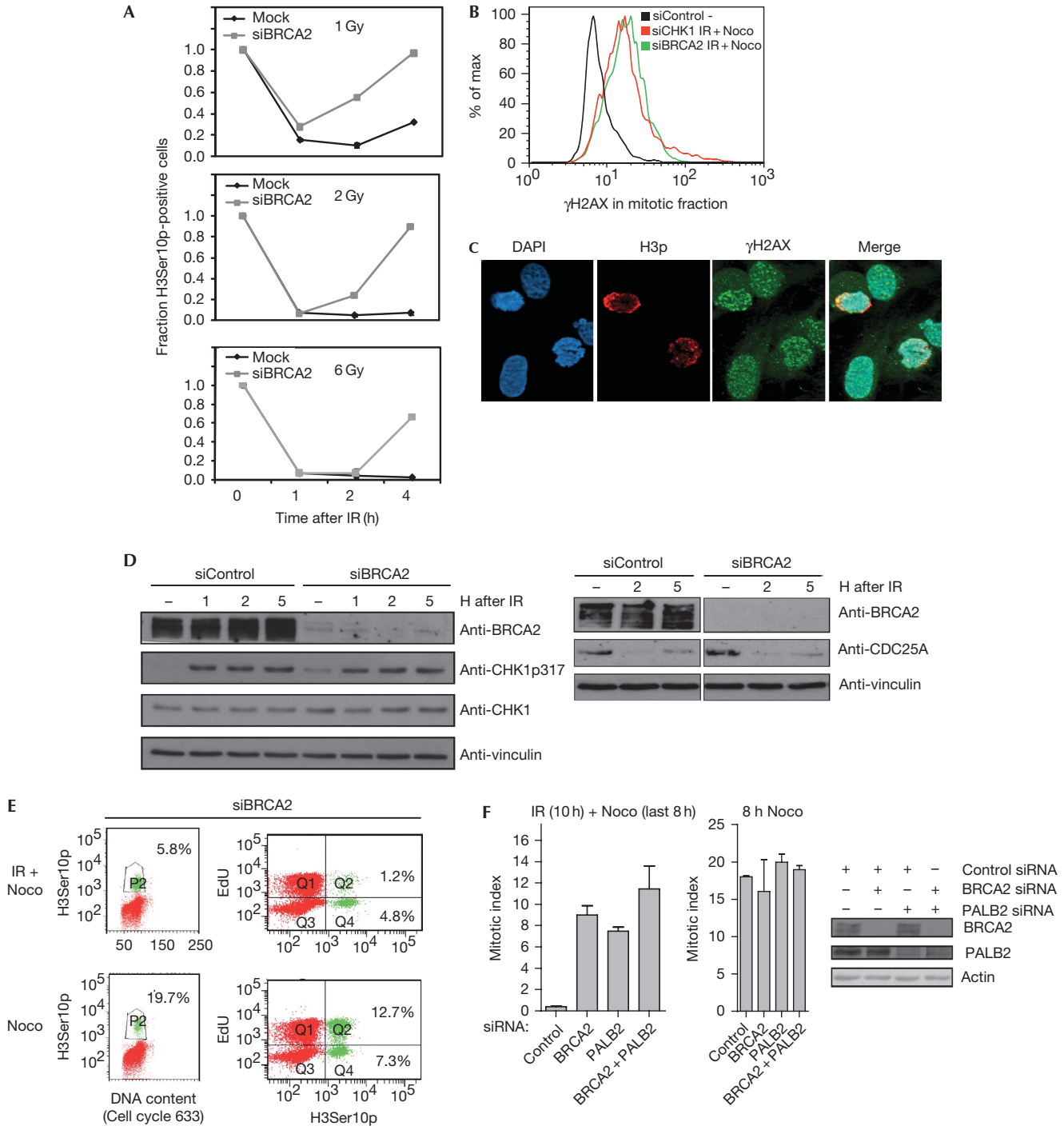

Fig 3 | For caption please see page 710.

supporting the idea that BRCA2 regulates the checkpoint response of cells in G2 phase (supplementary Fig S3 online).

PALB2 is a direct interactor of BRCA2 and thereby involved in BRCA2 functions during homologous recombination repair (Buisson *et al*, 2010; Dray *et al*, 2010). PALB2 was not included in the siRNA library used in our siRNA screens. However, independent experiments showed that the G2 checkpoint was abrogated by PALB2 downregulation (Fig 3F). Moreover, co-depletion of BRCA2 and PALB2 did not lead to additive checkpoint effects, indicating that BRCA2 and PALB2 function in the same pathway (Fig 3F). As the two proteins exert their role in homologous recombination repair by recruiting RAD51 to single-stranded DNA, we reasoned that RAD51 depletion might also lead to checkpoint abrogation. In fact, a recent report showed that mutations in the carboxy-terminus of BRCA2 caused faster mitotic entry and more rapid disassembly of RAD51, suggesting

◀ **Fig 3** | BRCA2 and PALB2 are required for the maintenance of the ionizing-radiation-induced G2/M checkpoint. (**A**) Flow cytometric analysis of U2OS p53dneg cells transfected with siRNA targeting BRCA2 at 0–4 h after 1, 2 or 6 Gy of IR treatment. The relative mitotic fraction was calculated by the number of H3Ser10p-positive cells relative to non-irradiated cells after IR. The plot is the mean of the percentage of H3Ser10p-positive cells of two experiments. (**B**) Flow cytometric analysis of U2OS p53dneg cells as described in Fig 2D. In addition, cells were stained for γH2AX. The histogram displays the γH2AX signal within the H3Ser10p-positive population. (**C**) Immunofluorescence images of U2O2 p53dneg cells transfected with BRCA2 siRNA. Cells were treated with IR (6 Gy) 2 days after transfection and stained with the indicated antibodies at 8 h after 6 Gy of IR. (**D**) Immunoblot of cells depleted for BRCA2 for 2 days and collected at 1, 2 and 5 h after 6 Gy of IR. Vinculin antibody was used as a loading control. (**E**) U2OS p53dneg cells were transfected with BRCA2 siRNA for 2 days and pulsed with EdU for 10 min before IR treatment (6 Gy). After 2 h of IR, nocodazole was added for 8 h and cells were collected for flow cytometry. Numbers are the percentage of H3Ser10p-positive cells of the whole population (left) and of the EdU-positive and EdU-negative population (right), respectively. (**F**) Flow cytometric analysis of U2OS p53dneg cells 2 days after transfection with siRNA targeting BRCA2, PALB2 and both siRNAs combined for 2 days. Where indicated, cells were treated with IR (6 Gy) and 2 h later with nocodazole for 8 h. Cells were collected and the mitotic index was analysed by flow cytometry using H3Ser10p antibody. The bar plot is the mean of the percentage of H3Ser10p-positive cells of three experiments. The knockdown efficiency was determined by immunoblotting. DAPI, 4,6-diamidino-2-phenylindole; IR, ionizing radiation; Noco, nocodazole; siRNA, short-interfering RNA; U2OS p53dneg, p53 dominant-negative U2OS.

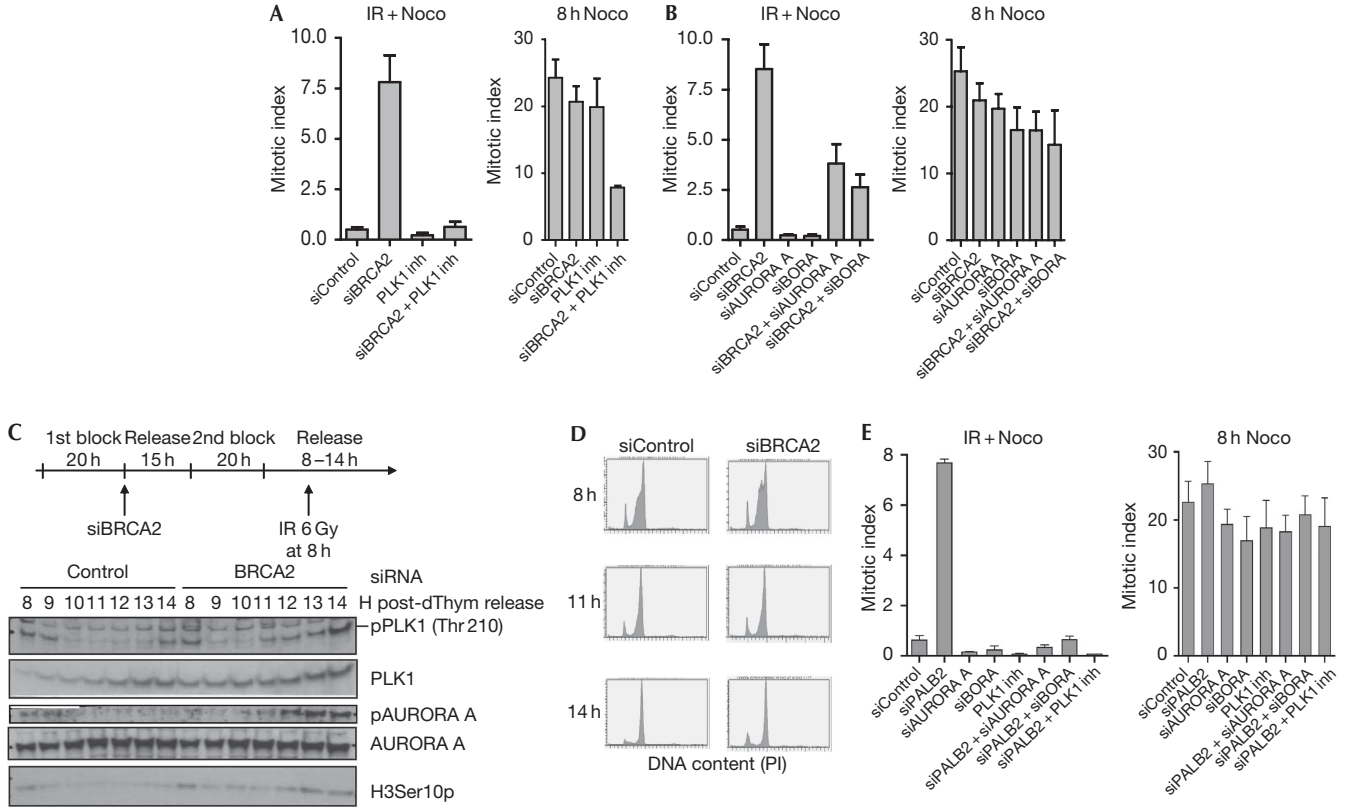

Fig 4 | BRCA2/PALB2 maintain the G2 checkpoint by control of the AURORA-A/BORA/PLK1 pathway. (**A**) Flow cytometric analysis of U2OS p53dneg cells transfected with siRNA targeting BRCA2 for 2 days. The cells were irradiated with 6 Gy of IR and 2 h later treated with nocodazole for 8 h. The PLK1 inhibitor BI2536 was added 30 min after IR. Cells were collected and the mitotic index was analysed by flow cytometry using H3Ser10p antibody. Error bars indicate s.e.m. ($n = 5$). (**B**) Flow cytometric analysis of U2OS p53dneg cells co-transfected with siRNA targeting BRCA2, AURORA A and BORA for 2 days. The cells were treated and analysed as in **A**. Error bars indicate s.e.m. ($n = 4$). (**C**) PLK1 and AURORA A are activated prematurely after IR in synchronized BRCA2-depleted cells. U2OS p53dneg cells were synchronized by double thymidine block and transfected with siRNA targeting BRCA2 after release from the first block. Eight hours after the second release, cells were treated with 6 Gy of IR and collected at 1 h intervals thereafter (top). Protein lysates were subjected to immunoblotting with the indicated antibodies (bottom). (**D**) Flow cytometry analysis of parallel samples from the same experiment as in **C**. Cells were stained with Hoechst and DNA profiles are shown. (**E**) Flow cytometric analysis of U2OS p53dneg cells transfected with siRNA targeting PALB2, AURORA A and BORA for 2 days. The cells were irradiated with 6 Gy of IR and 2 h later treated with Nocodazole for 8 h. Where indicated, the PLK1-inhibitor BI2536 was added 30 min after IR. Cells were collected and the mitotic index was analysed by flow cytometry using H3Ser10p antibody. Error bars indicate s.e.m. ($n = 3$). inh, inhibitor; IR, ionizing radiation; siRNA, short-interfering RNA; U2OS p53dneg, p53 dominant-negative U2OS.

a link between completion of DNA repair and the cell cycle (Ayoub *et al*, 2009). However, we found that depletion of RAD51 did not cause abrogation of the G2 checkpoint (supplementary Fig S4 online), suggesting that BRCA2 and PALB2 regulate G2 checkpoint maintenance independently of RAD51, as well as the completion of homologous recombination repair.

Checkpoint recovery is an active process to resume the cell cycle following checkpoint arrest, which depends on the AURORA A/BORA/PLK1 network (Macurek *et al*, 2008). To investigate whether PLK1 is involved in premature recovery following BRCA2 depletion, we examined the effects of adding a PLK1 inhibitor after exposure to ionizing radiation. Inhibition of PLK1 counteracted the G2 checkpoint abrogation of BRCA2-depleted cells, although knockdown of BRCA2 and PLK1 inhibition also had an inhibitory effect on mitotic entry in the absence of ionizing radiation (Fig 4A). When comparing the numbers of cells that entered mitosis after damage (ionizing radiation + nocodazole treatment) with the number of cells that entered mitosis without damage (Nocodazole treatment), PLK1 inhibition caused a fivefold reduction of the mitotic index in BRCA2-depleted cells (Fig 4A). Furthermore, codepletion of BRCA2 with AURORA A and BORA, respectively, reduced the number of cells that entered mitosis after exposure to ionizing radiation, compared with BRCA2 knockdown alone (Fig 4B; supplementary Fig S5 online).

During checkpoint recovery, PLK1 becomes activated by AURORA A/BORA-mediated phosphorylation on T210 (Tsvetkov & Stern, 2005; Macurek *et al*, 2008; Seki *et al*, 2008), and because of reaccumulation of stabilized PLK1 (Bassermann *et al*, 2008). In the absence of BRCA2, PLK1 was phosphorylated at earlier time points after exposure to ionizing radiation (Fig 4C,D). Moreover, AURORA A autophosphorylation, a prerequisite for AURORA A activity (Walter *et al*, 2000), occurred earlier after exposure to ionizing radiation in the absence of BRCA2 (Fig 4C). Importantly, BORA, AURORA A and PLK1 ablation also restored the G2 checkpoint in PALB2-depleted cells (Fig 4E; supplementary Fig S5 online), and PLK1 phosphorylation occurred at earlier time points after exposure to ionizing radiation in the absence of PALB2 (supplementary Fig S6 online). Together, these results suggest that BRCA2 and PALB2 are required to maintain the AURORA A/BORA/PLK1 pathway in an inactive state after exposure to ionizing radiation to prevent cells with DNA damage from entering mitosis prematurely. In the presence of BRCA2, U2OS cells treated with 6 Gy of ionizing radiation will finally enter mitosis at 20–30 h after exposure to ionizing radiation. This occurs in a PLK1-dependent manner (Syljuåsen *et al*, 2006). On the basis of our results, we propose that the inactivation of BRCA2/PALB2 suppression of PLK1 is involved in causing such mitotic entry. It remains to be elucidated how BRCA2 and PALB2 regulate AURORA A/BORA/PLK1, and how BRCA2/PALB2-dependent control of the PLK1 pathway is turned off to allow cell-cycle progression. Notably, BRCA2 was reported to interact with PLK1 in mitosis (Lin *et al*, 2003), and it is possible that protein interactions between BRCA2/PALB2 and AURORA A/BORA/PLK1 are involved in the regulation of checkpoint maintenance.

In conclusion, we have used the siRNA-screen approach to uncover new roles for key regulators of biologically important pathways. We show for the first time that the homologous recombination repair proteins BRCA2 and PALB2 are required for G2 checkpoint maintenance and, importantly, that their function seems to be independent of homologous recombination, as RAD51 depletion does not affect G2 checkpoint control. This new checkpoint function might contribute to BRCA2 and PALB2 tumour-suppressor functions and influence responses to cancer therapy.

METHODS

Cell culture, chemicals and irradiation. Human U2OS osteosarcoma cells, TIG3 telomerized human fetal lung fibroblasts, HeLa cervical and HCT116 $p53^{-/-}$ colorectal cells were grown in DMEM medium (Invitrogen) with 10% fetal bovine serum. U2OS cells expressing a dominant-negative p53 in a tet-off system (U2OS p53dneg) were grown in DMEM with 10% fetal bovine serum and 1 ng/ml doxycycline. For expressing the dominant-negative p53, U2OS p53dneg cells were washed twice in PBS and grown in the absence of doxycycline. For siRNA-mediated knockdown, cells were transfected using oligofectamine (Invitrogen) or lipofectamine RNAiMAX (Invitrogen) according to the manufacturer's protocol. Oligonucleotide sequences and double thymidine synchronization are described in the supplementary information online. CHK1-inhibitor Gö6976 (Calbiochem) was used at 100 nM, and PLK1-inhibitor BI 2536 (Axon) at 200 nM. Nocodazole (Sigma-Aldrich) was used at 100 ng/ml. Ionizing radiation was delivered by X-ray generators (Faxitron CP160, 160 kV, 6.3 mA and Faxitron RX650, 130 kV, 3 mA).

Robot-automated screen. Detailed procedures are described in the supplementary information online.

Antibodies. The following antibodies were used: BRCA2 (Ab-1, Calbiochem, 1:1,000), phospho-AURORA (pAurABC #2914, Cell Signalling, 1:1,000), AURORA A (ab1287, Abcam, 1:1,000), phospho-PLK1-T210 (Phospho-PLK1 activation kit, Thermo Scientific, 1:1,000), PLK1 (H152, Santa Cruz, 1:500), PALB2 (Bethyl Laboratories, 1:1,000), anti-BORA (gift from Erich Nigg), Cdc25a (SC7389, Santa Cruz, 1:50), CHK1-S317p (2344 L cell signalling), CHK1-S345p (cell signalling) vinculin (V9131, Sigma, 1:10,000), actin (AB1501, Abcam) and MCM7 (DCS-141; Sørensen *et al* (2005), 1:50).

Immunoblotting, flow cytometry and immunofluorescence. Cells were prepared for immunoblotting, flow cytometry and immunofluorescence as described previously (Jørgensen *et al*, 2007) and in the supplementary information online.

Supplementary information is available at EMBO *reports* online (http://www.emboreports.org).

ACKNOWLEDGEMENTS

This work was supported by The Novo Nordisk Foundation, The Danish Cancer Society, The Lundbeck Foundation, The Danish Medical Research Council, The Norwegian Cancer Society, The Norwegian Research Council, Radiumhospitalets Legater and The South-Eastern Norway Health Authority. We are grateful to E. Nigg for his gift of BORA antibody.

CONFLICT OF INTEREST

The authors declare that they have no conflict of interest.

REFERENCES

Ayoub N, Rajendra E, Su X, Jeyasekharan AD, Mahen R, Venkitaraman AR (2009) The carboxyl terminus of Brca2 links the disassembly of Rad51 complexes to mitotic entry. *Curr Biol* **19:** 1075–1085

Bassermann F, Frescas D, Guardavaccaro D, Busino L, Peschiaroli A, Pagano M (2008) The Cdc14B–Cdh1–Plk1 axis controls the G2 DNA-damage-response checkpoint. *Cell* **134:** 256–267

Birmingham A *et al* (2009) Statistical methods for analysis of high-throughput RNA interference screens. *Nat Methods* **6:** 569–575

Bonner WM, Redon CE, Dickey JS, Nakamura AJ, Sedelnikova OA, Solier S, Pommier Y (2008) γH2AX and cancer. *Nat Rev Cancer* **8:** 957–967

Boutros R, Dozier C, Ducommun B (2006) The when and wheres of CDC25 phosphatases. *Curr Opin Cell Biol* **18:** 185–191

Buisson R, Dion-Cote AM, Coulombe Y, Launay H, Cai H, Stasiak AZ, Stasiak A, Xia B, Masson JY (2010) Cooperation of breast cancer proteins PALB2 and piccolo BRCA2 in stimulating homologous recombination. *Nat Struct Mol Biol* **17:** 1247–1254

Ciccia A, Elledge SJ (2010) The DNA damage response: making it safe to play with knives. *Mol Cell* **40:** 179–204

Deckbar D, Birraux J, Krempler A, Tchouandong L, Beucher A, Walker S, Stiff T, Jeggo P, Lobrich M (2007) Chromosome breakage after G2 checkpoint release. *J Cell Biol* **176:** 749–755

Dray E *et al* (2010) Enhancement of RAD51 recombinase activity by the tumor suppressor PALB2. *Nat Struct Mol Biol* **17:** 1255–1259

Hendzel MJ, Wei Y, Mancini MA, Van Hooser A, Ranalli T, Brinkley BR, Bazett-Jones DP, Allis CD (1997) Mitosis-specific phosphorylation of histone H3 initiates primarily within pericentromeric heterochromatin during G2 and spreads in an ordered fashion coincident with mitotic chromosome condensation. *Chromosoma* **106:** 348–360

Hu B, Wang H, Wang X, Lu HR, Huang C, Powell SN, Huebner K, Wang Y (2005) Fhit and CHK1 have opposing effects on homologous recombination repair. *Cancer Res* **65:** 8613–8616

Iliakis G, Wang Y, Guan J, Wang H (2003) DNA damage checkpoint control in cells exposed to ionizing radiation. *Oncogene* **22:** 5834–5847

Jørgensen S, Elvers I, Trelle MB, Menzel T, Eskildsen M, Jensen ON, Helleday T, Helin K, Sørensen CS (2007) The histone methyltransferase SET8 is required for S-phase progression. *J Cell Biol* **179:** 1337–1345

König R *et al* (2007) A probability-based approach for the analysis of large-scale RNAi screens. *Nat Methods* **4:** 847–849

Lin HR, Ting NS, Qin J, Lee WH (2003) M phase-specific phosphorylation of BRCA2 by Polo-like kinase 1 correlates with the dissociation of the BRCA2-P/CAF complex. *J Biol Chem* **278:** 35979–35987

Macurek L, Lindqvist A, Lim D, Lampson MA, Klompmaker R, Freire R, Clouin C, Taylor SS, Yaffe MB, Medema RH (2008) Polo-like kinase-1 is activated by aurora A to promote checkpoint recovery. *Nature* **455:** 119–123

Seki A, Coppinger JA, Jang CY, Yates JR, Fang G (2008) Bora and the kinase Aurora a cooperatively activate the kinase Plk1 and control mitotic entry. *Science* **320:** 1655–1658

Syljuåsen RG, Jensen S, Bartek J, Lukas J (2006) Adaptation to the ionizing radiation-induced G2 checkpoint occurs in human cells and depends on checkpoint kinase 1 and Polo-like kinase 1 kinases. *Cancer Res* **66:** 10253–10257

Sørensen CS, Hansen LT, Dziegielewski J, Syljuåsen RG, Lundin C, Bartek J, Helleday T (2005) The cell-cycle checkpoint kinase Chk1 is required for mammalian homologous recombination repair. *Nat Cell Biol* **7:** 195–201

Sørensen CS, Melixetian M, Klein DK, Helin K (2010) NEK11: linking CHK1 and CDC25A in DNA damage checkpoint signaling. *Cell Cycle* **9:** 450–455

Tsvetkov L, Stern DF (2005) Phosphorylation of Plk1 at S137 and T210 is inhibited in response to DNA damage. *Cell Cycle* **4:** 166–171

van Vugt MA, Bras A, Medema RH (2004) Polo-like kinase-1 controls recovery from a G2 DNA damage-induced arrest in mammalian cells. *Mol Cell* **15:** 799–811

van Vugt MA, Bras A, Medema RH (2005) Restarting the cell cycle when the checkpoint comes to a halt. *Cancer Res* **65:** 7037–7040

Venkitaraman AR (2009) Linking the cellular functions of BRCA genes to cancer pathogenesis and treatment. *Annu Rev Pathol* **4:** 461–487

Walter AO, Seghezzi W, Korver W, Sheung J, Lees E (2000) The mitotic serine/threonine kinase Aurora2/AIK is regulated by phosphorylation and degradation. *Oncogene* **19:** 4906–4916